Electronic Supplementary Material (ESI) for Inorganic Chemistry Frontiers.

Supporting Information

Economically palladium decorated on m-aminophenol-formaldehyde derived porous carbon spheres for enhanced catalytic reduction of organic dyes†

Pitchaimani Veerakumar,[*,a,b] **I. Panner Muthuselvam,**[c] **Pounraj Thanasekaran,**[d] **and King-Chuen Lin,**[*,a,b]

[a]*Department of Chemistry, National Taiwan University, Taipei 10617, Taiwan*

[b]*Institute of Atomic and Molecular Sciences, Academia Sinica, Taipei 10617, Taiwan*

[c]*Department of Materials Science, Central University of Tamil Nadu, Neelakudi, Thiruvarur 610005, India*

[d]*Institute of Chemistry, Academia Sinica, Taipei 11529, Taiwan*

Corresponding Authors

*E-mail: spveerakumar@gmail.com (P. Veerakumar).

*E-mail: kclin@ntu.edu.tw (K.-C. Lin).

1. Materials and Chemicals. Palladium acetylacetonate ($Pd(acac)_2$, ≥99.9%), sodium borohydride ($NaBH_4$, 99.99%), crystal violet (CV), eosin yellow (EY) and sunset yellow FCF (SY) were purchased from sigma-aldrich and used without further purification. m-aminophenol (ACS, 99.98%) and formaldehyde (37% in water) were purchased from Acros. All other chemicals used were analytical grade, and all solutions were prepared using ultrapure water (Millipore).

2. Catalyst characterization. Powder X-ray diffraction (XRD) measurements were performed on the PANalytical (X'Pert PRO) instrument using a Cu Kα radiation (λ = 0.1541 nm). The morphology of this composite was examined by a field-emission transmission electron microscopy (FE-TEM; JEOL JEM-2100F). The palladium content of Pd@PCS sample was determined by means of inductively coupled plasma atomic emission spectroscopy (ICP-AES) using a PerkinElmer Optima 5300 DV instrument. N_2 adsorption/desorption isotherms were measured using a physisorption apparatus (Micromeritics, ASAP 2020). All Fourier-transform infrared (FT-IR) spectra were recorded by a Bruker IFS28 spectrometer in the region of 4000–400 cm^{-1} with a spectral resolution of 2 cm^{-1} using KBr pellet method at room temperature. Thermogravimetric and differential thermal analysis (TG-DTA) measurements were performed on a Netzsch TG-209 instrument under air atmosphere. Ultraviolet visible (UV-vis) spectroscopy was conducted on a Thermo Scientific evolution 220 spectrophotometer.

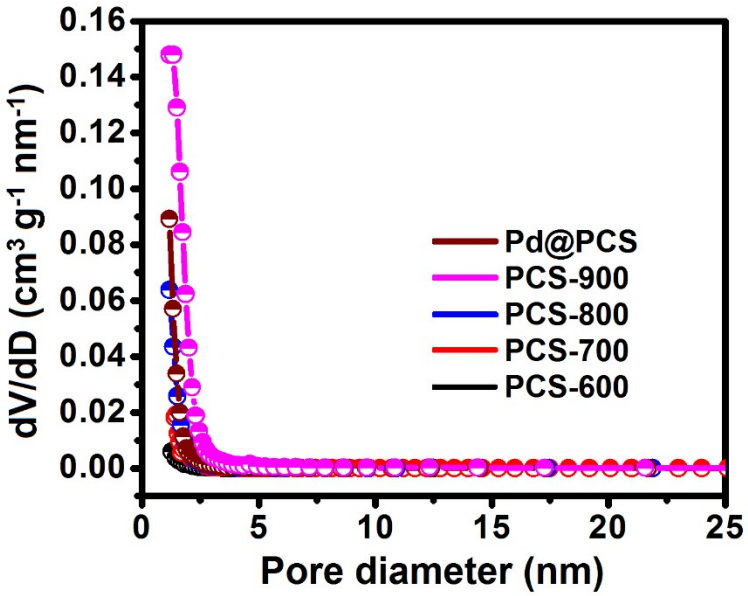

Fig. S1. DFT pore size distributions of as-prepared PCSs and Pd@PCS catalysts.

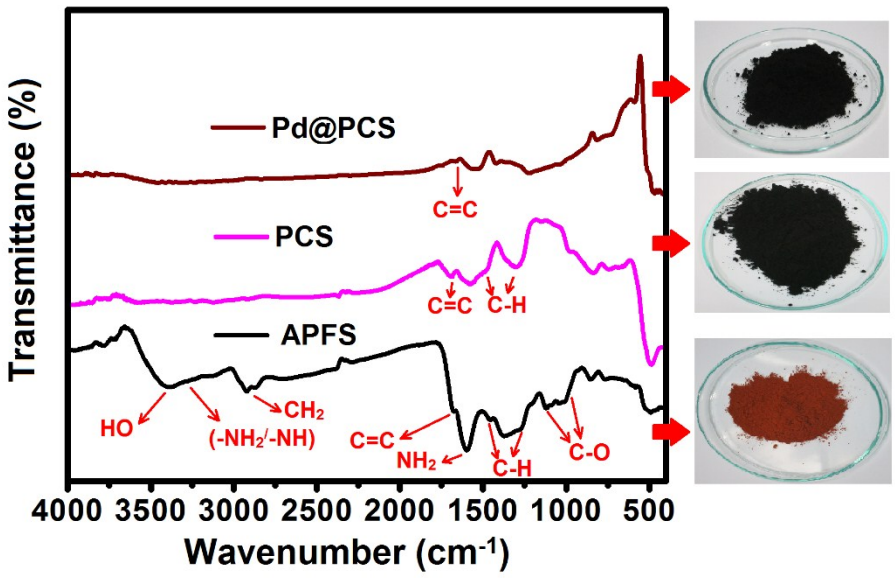

Fig. S2. FTIR spectra of APFS, PCS, and Pd@PCS catalysts and their corresponding photographs (Inset on right).

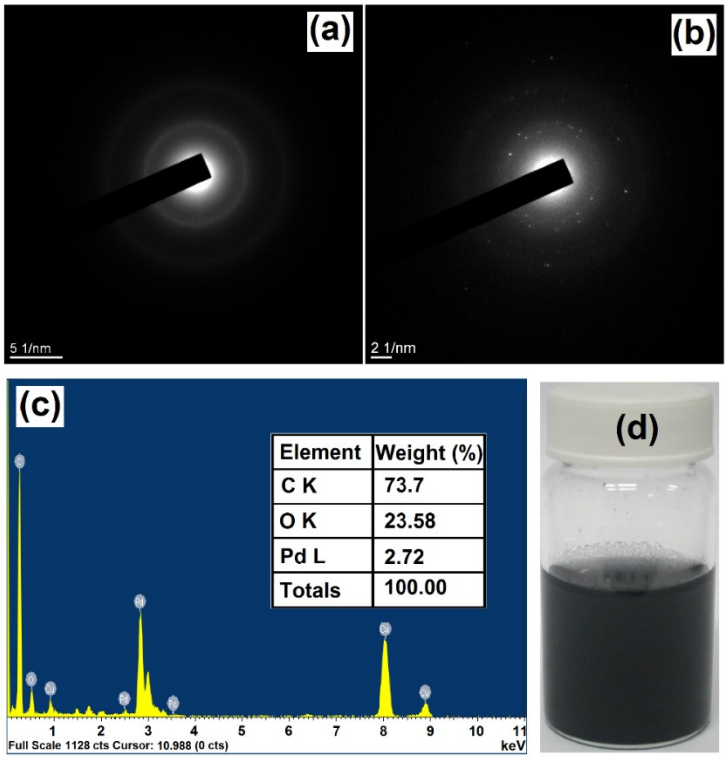

Fig. S3. (a,b) SAED patterns of PCS-900 and Pd@PCS catalysts, (c) EDX profile and (d) Pd@PCS catalyst dispersed in DI water.

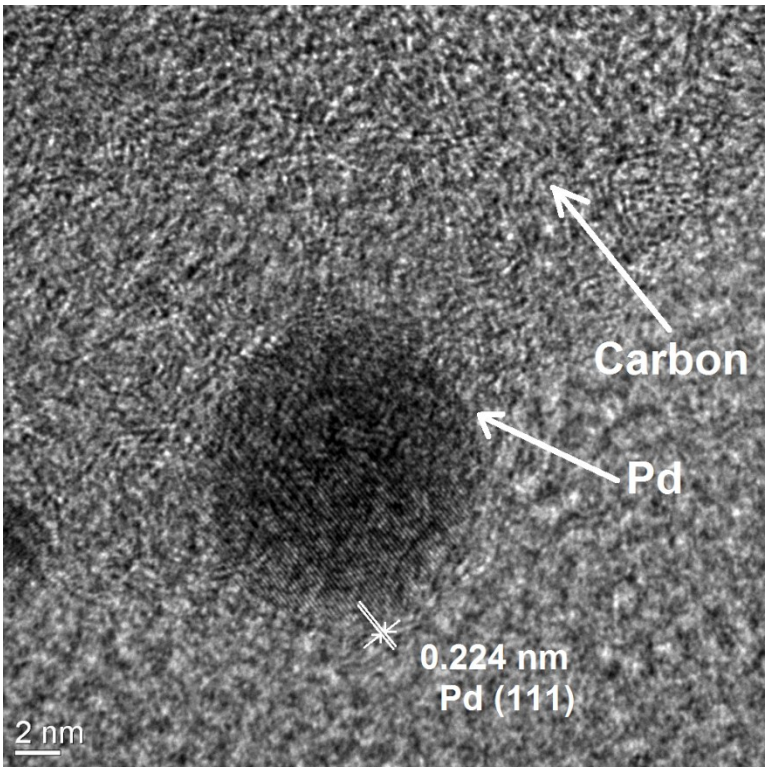

Fig. S4. The FETEM image of the Pd NPs decorated PCS support showing lattice fringe corresponding to Pd (111) plane with d-spacing line (d = 0.224 nm).

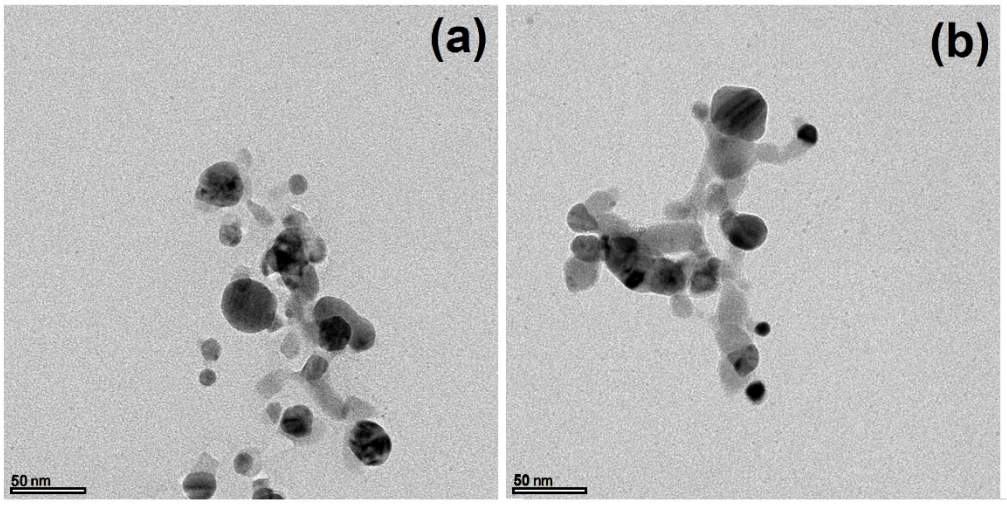

Fig. S5. (a, b) TEM images of Pd NPs.

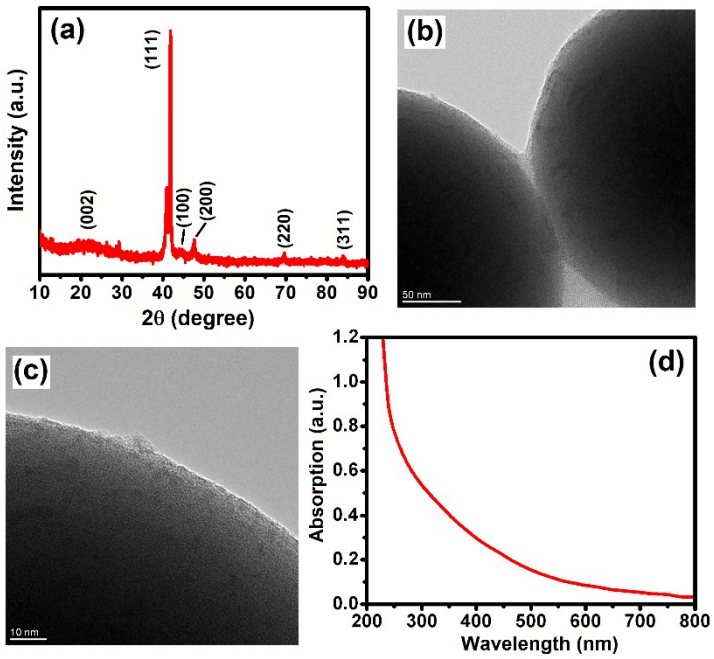

Fig. S6. (a) XRD pattern, (b,c) TEM images and (d) UV–Vis absorption spectrum of Pd@PCS catalyst after spent five runs.

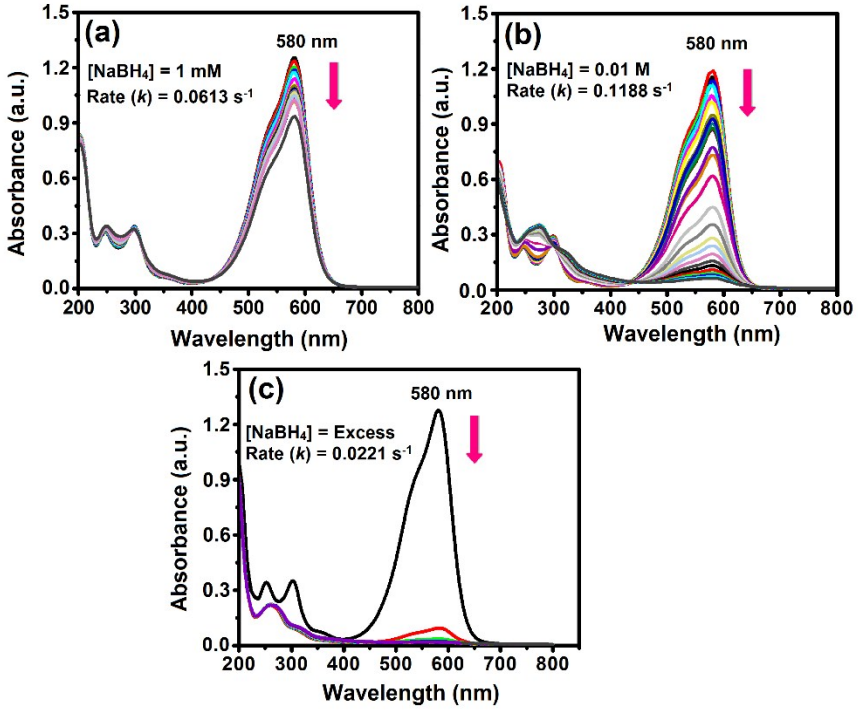

Fig. S7. UV-visible absorption spectra of CV reduction in the addition of $NaBH_4$ (a) 0.001M, (b) 0.01M and, (c) an excess amount of $NaBH_4$.

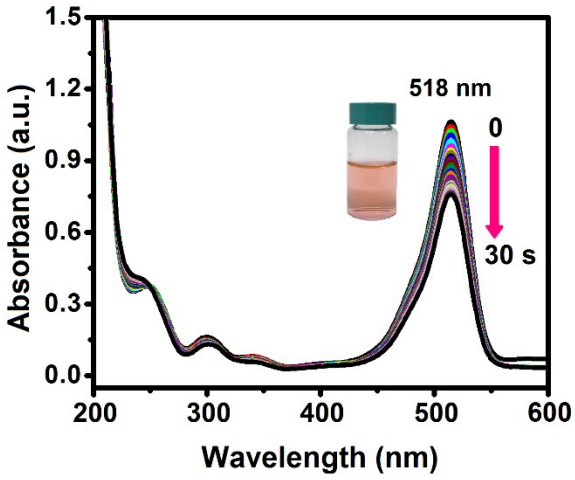

Fig. S8. UV-vis absorption spectra for the reduction of EY over the PCS-900 catalyst.

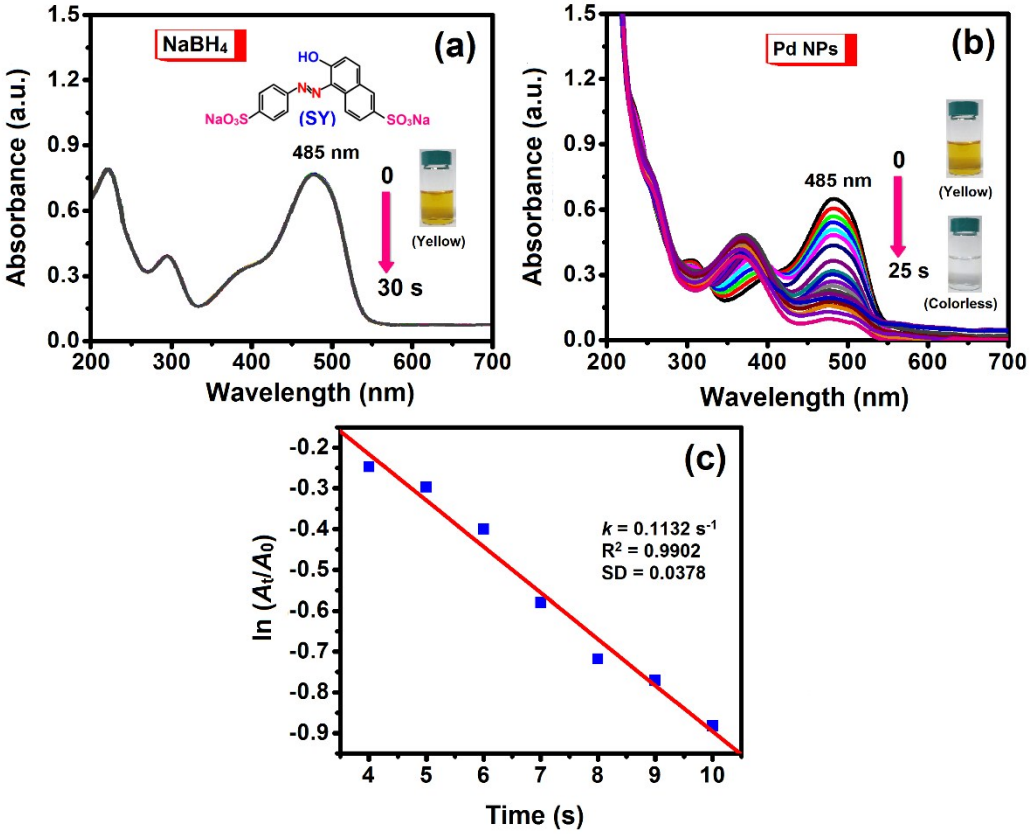

Fig. S9. (a) UV-Visible absorption spectra of SY by $NaBH_4$ in the absence of Pd@PCS catalyst, (b) presence of Pd NPs as a catalyst (inside the photographs of SY before and after reduction) and (c) its corresponding plot $\ln(A_t/A_0)$ *vs.* time.

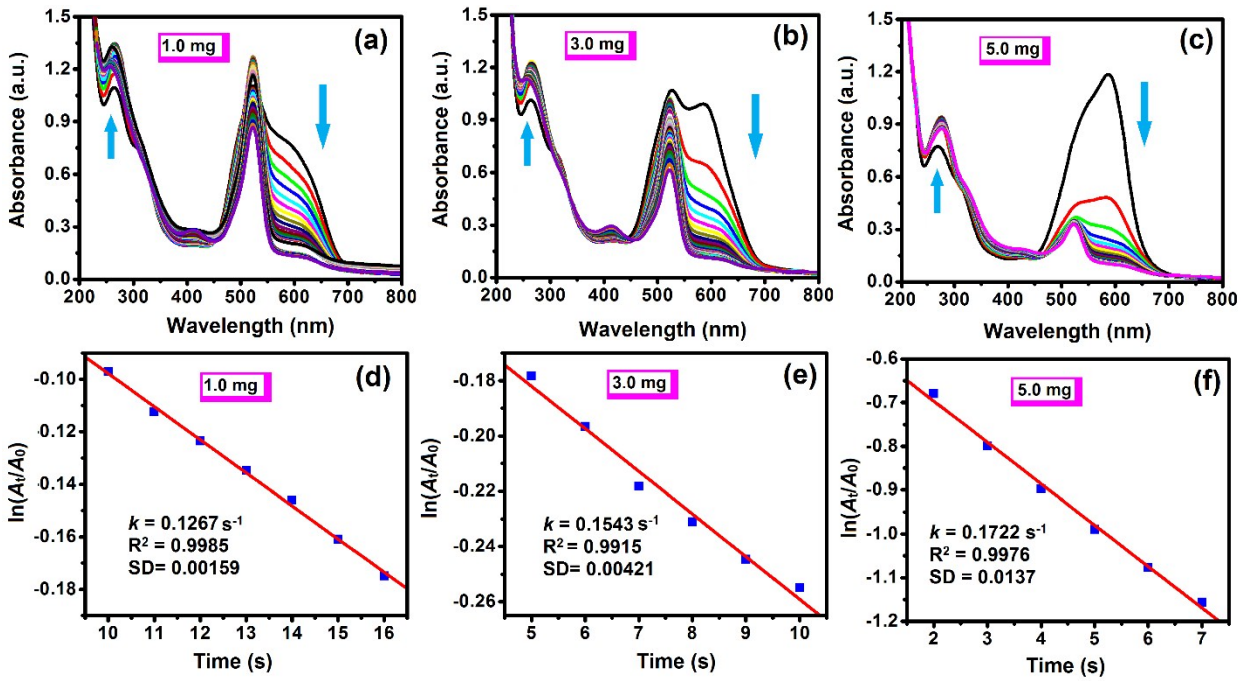

Fig. S10. UV–visible spectra representing the simultaneous reduction of a mixture of CV and EY dyes in the presence of Pd@PCS catalyst (a) 1 mg, (b) 3 and (c) 5 mg mL^{-1} under the identical experimental conditions, and (d-f) their corresponding plot of $\ln A_t/A_0$ *vs* time.

Table S1. The recycling ability of Pd@PCS catalyst for the reduction of CV dye.

No. of runs	Fresh	1st run	2nd run	3rd run	4th run	5th run
k (s^{-1})	0.2301	0.2284	0.2245	0.2183	0.2126	0.2101

Table S2. Comparison of the catalytic activity of various nanomaterials for the reduction of CV dye.

Catalyst	Size (nm)	Time (s)	Method	Source/ reductant	S_{BET} (m^2 g^{-1})/ V_{Tot} (cm^3 g^{-1})	Rate constant (k, s^{-1})	Reference
CdS/Zeolite A	48–68	1500	PD[i]	Sun-light	NR	NR[l]	1
$CuFe_2O_4$	50–100	5400	MR[j]	NR	NR	5.7×10^{-2}	2
Sm_2InTaO_7	>500	3600	PD	UV lamp	NR	NR	3
Fe/AC[a]	250–300	1800	Ozonation	O_3[k]	195.0/0.1645	NR	4
Ru/CPM-1[b]	2.6±0.5	30	Reduction	$NaBH_4$	1416/1.095	0.2041	5
Ru/CPM-2	2.8±0.5	30	Reduction	$NaBH_4$	1313/0.988	0.2436	5
PS-PVBC-g-PAC[c] AgNPs	20–25	30	Reduction	$NaBH_4$	NR	1.674×10^5	6
PS-PVBC-g-PAC PdNPs	20–25	30	Reduction	$NaBH_4$	NR	8.45×10^4	6
PS-PVBC-g-PAC AuNPs	20–25	30	Reduction	$NaBH_4$	NR	2.546×10^5	6
Fe_3O_4@C-dot[d]/Ag	6.1	75	Reduction	$NaBH_4$	NR	4.354×10^{-2}	7
GO[e]/Ru NCs[f]	NR	1800	Reduction	$NaBH_4$	NR	4.6×10^{-3}	8
GO/Ag NCs[g]	NR	1800	Reduction	$NaBH_4$	NR	5.0×10^{-3}	8
GO/Pd NCs[h]	NR	1800	Reduction	$NaBH_4$	NR	4.8×10^{-3}	8
GO/Ru–Ag NCs	6	1800	Reduction	$NaBH_4$	NR	5.8×10^{-3}	8
GO/Ru–Pd NCs	8.9	1800	Reduction	$NaBH_4$	NR	5.5×10^{-3}	8
Pd@PCS (1.0 mg)	12 ± 0.8	20	Reduction	$NaBH_4$	896.3/0.934	0.2031	This work
Pd@PCS (2.0 mg)	12 ± 0.8	20	Reduction	$NaBH_4$	896.3/0.934	0.2355	This work
Pd@PCS (3.0 mg)	12 ± 0.8	20	Reduction	$NaBH_4$	896.3/0.934	0.2389	This work

[a]Activated carbon. [b]Carbon porous materials. [c]Poly(styrene)-co-(vinyl benzyl chloride) grated 2-acryloxyethyltrimethyl ammonium chloride. [d]Carbon dots. [e]Graphene oxide. [f]Ruthenium nanocomposites. [g]Silver nanocomposites. [h]Palladium nanocomposites. [i]Photo degradation. [J]Microwave radiation. [k]Ozone. [l]Not reported.

Table S3. Comparison of the catalytic activity of various nanocatalysts for the reduction of EY dye.

Catalyst	Size (nm)	Time (min)	Reductant	Rate constant (k)	S_{BET} (m^2 g^{-1})/ V_{Tot} (cm^3 g^{-1})	Reference
Ag NPs	18–24	8	$NaBH_4$	0.3659 min^{-1}	NR	9
Ag–NSs[a]	20	100 s	$NaBH_4$	7.001×10^{-3} s^{-1}	NR	10
p(MAc)[b]–Cu	>50	12	$NaBH_4$	0.004 ± 0.00007 s^{-1}	NR	11
Co–ZrO_2[c]–MWCNTs[d]	8	180	Photoreduction	16.86×10^{-3} min^{-1}	NR	12
PAGNPs[e]	28 ± 5.6	12	$NaBH_4$	NR	NR	13
Ag Colloids	22	10	$NaBH_4$	0.2312 min^{-1}	NR	14
Au–Ag NPs	9.2 ± 0.3	20	NADH[m]	14.72×10^{-3} s^{-1}	NR	15
Chitosan–Au NPs	25	30	$NaBH_4$	8×10^{-3} s^{-1}	NR	16
SiNW[f]/Pd NPs	3–9	24	$NaBH_4$	0.06943 ± 0.00135.	NR	17
Au NRs[g]	>50	NR[n]	$NaBH_4$	NR	2294.47 (nm^2)/6960.47 (nm^3)	18
Cu_2O NPs	85 ± 5	9	$NaBH_4$	NR	NR	19
rGO[h]–AuNFs[i]	>200	18	$NaBH_4$	NR	NR	20
AOT[j]–Au NFs	>200	300s	$NaBH_4$	1.49×10^{-2} s^{-1}	NR	21
Hollow Cu–spheres	5–10 μm	30	$NaBH_4$	NR	NR	22
p(TA)[k]–Co ILs[l]	5–10	40	$NaBH_4$	0.07	NR	23
p(TA)–Ni ILs	5–10	60	$NaBH_4$	0.05	NR	23
p(TA)–Cu ILs	5–10	9.66	$NaBH_4$	0.2	NR	23
Fe_3O_4@SiO_2-Ag NPs	48 ± 2	13.5	$NaBH_4$	0.2367 min^{-1}	NR	24
Hollow Au–spheres	35 ± 6	NR	$NaBH_4$	NR	NR	25
Fe_3O_4@Nico@Cu	>100	9	$NaBH_4$	0.22 min^{-1}	NR	26
Pd@PCS	12 ± 0.8	20 s	$NaBH_4$	0.1223 s^{-1}	896.3/0.934	This work

[a]Nanoshells. [b]Poly(methacrylic acid) microgels. [c]Ziconia oxide. [d]Multiwalled carbon nanotubes. [e]Plumeria alba with gold nanoparticles. [f]Silicon nanowires. [g]Gold nanorods. [h]Reduced graphene oxide. [i]Gold nanoflowers. [j]Sodium bis(2-ethylhexyl)sulphosuccinate). [k]Poly(tannic acid). [l]Ionic liquids. [m]Dihydronicotinamide adenine dinucleotide. [n]Not reported.

3. References

(1) A. N. Ejhieh and Z. Banan, *Desalination* 2011, **279**, 146–151.

(2) H. Chen, S. Yang, J. Chang, K. Yu, D. Li, C. Sun and A. Li, *Chemosphere* 2012, **89**, 185–189.

(3) L. M. Torres-Marıtnez, E. Moctezuma, M. A. Ruiz-Gomez, I. Juarez-Ramırez and M. Z. Figueroa-Torres, *Res. Chem. Intermed.* 2013, **39**, 1533–1544.

(4) J. Wu, H. Gao, S. Yao, L. Chen, Y. Gao and H. Zhang, *Sep. Purif. Technol.* 2015, **147**, 179–185.

(5) P. Veerakumar, N. Dhenadhayalan, K.-C. Lin and S.-B. Liu, *J. Mater. Chem. A* 2015, **3**, 23448–23457.

(6) E. Murugan and P. Shanmugam, *Bull. Mater. Sci.* 2015, **38**, 629–637.

(7) Y. Guo, D. Tang, L. Zhang, B. Li, A. Iqbal, W. Liu, W. Qin, *Ceramics Inter.* 2017, **43**, 7311–7320.

(8) K. Sivaranjan, P. Vanitha, A. Sathiyaseelan, P. T. Kalaichelvan, M. Sathuvan, R. Rengasamy and J. Santhanalakshmi, *New J. Chem.* 2017, **41**, 4348–4359.

(9) A. Rajan, V. Vilas and D. Philip, *J. Mol. Liq.* 2015, **207**, 231–236.

(10) B. Vellaichamy and P. Periakaruppan, *RSC Adv.* 2016, **6**, 31653–31660.

(11) M. Ajmal, M. Siddiq, H. Al-Lohedan and N. Sahiner, *RSC Adv.* 2014, **4**, 59562–59570.

(12) W. W. Anku, S. O. Oppong, S. K. Shukla, E. S. Agorku and P. P. Govender, *Prog. Nat. Sci.: Mater. Inter.* 2016, **26**, 354–361.

(13) R. Mata, A. Bhaskaran and S. R. Sadras, *Particuology* 2016, **24**, 78–86.

(14) V. K. Vidhu and D. Philip, *Micron* 2014, **56**, 54–62.

(15) J. Santhanalakshmi and P. Venkatesan, *J. Nanopart. Res.* 2011, **13**, 479–490.

(16) A. Komalam, L. G. Muraleegharan, S. Subburaj, S. Suseela, A. Babu and S. George, *Inter. Nano Lett.* 2012, **2**, 26.

(17) F. Wang, M. Shao, L. Cheng, D. Chen, Y. Fu and D. D. D. Ma, *Mater. Res. Bull.* 2009, **44**, 126–129.

(18) G. Weng, Y. Qi, J. Li and J. Zhao, *J. Nanopart. Res* 2015, **17**, 367.

(19) R. Sahoo, S. Dutta, M. Pradhan, C. Ray, A. Roy, T. Pal and A. Pal, *Dalton Trans.* 2014, **43**, 6677–6683.

(20) M. Šimšíková, M. Bartoš, J. Čechala and T. Šikola, *Catal. Sci. Technol.* 2016, **6**, 3008–3017.

(21) S. Srivastava, S. K. Sharma and R. K. Sharma, *Colloids Surf A* 2011, **373**, 61–65.

(22) L. Xia, H. Zhao, G. Liu, X. Hu, Y. Liu, J. Li, D. Yang and X. Wang, *Colloids Surf A* 2011, **384**, 358–362.

(23) N. Sahiner, S. Sagbas and N. Aktas, *RSC Adv.* 2015, **5**, 18183–18195.

(24) L. Sun, J. He, S. An, J. Zhang, J. Zheng and D. Ren, *Chin. J. Catal.,* 2013, **34**, 1378–1385.

(25) M. A. Mahmoud and G. Weng, *Catal. Commun.* 2013, **38**, 63–66.

(26) M. Amir, U. Kurtan and A. Baykal, *Chin. J. Catal.* 2015, **36**, 1280–1286.